

Continuously tunable, high-power, single-mode radiation from a short-pulse free-electron laser

H. H. Weits and D. Oepts

FOM Instituut voor Plasmafysica "Rijnhuizen," P.O. Box 1207, 3430 BE Nieuwegein, The Netherlands

(Received 25 August 1998)

This paper gives the first demonstration of high-power, continuously tunable, narrowband radiation that is produced by means of a free-electron laser (FEL) in the far-infrared region of the electromagnetic spectrum. A Fox-Smith intracavity étalon was used to induce phase coherence between the 40 optical micropulses that were circulating in the laser cavity. The corresponding phase-locked spectrum consisted of a comb of discrete frequencies separated by 1 GHz. A pair of external Fabry-Pérot étalons was used to filter out a single line from this spectrum. The power in the selected narrow line at $69\mu\text{m}$ wavelength was equal to 250 mW during the macropulse of the laser. The spectral width of the selected line is as small as that of a single cavity mode, i.e., a fraction of 25 MHz, in single macropulses of the laser. The average bandwidth of 25 MHz is determined by mode hopping of the phase-locked FEL. The selected frequency hops over 25 MHz between the extrema of this band. The influence of partially coherent spontaneous emission and mode hopping on the final linewidth was studied. The narrow-linewidth radiation was scanned in frequency over 1 GHz. We show that the possibilities to scan over smaller or larger frequency intervals are unlimited. [S1063-651X(99)04607-3]

PACS number(s): 41.60.Cr, 42.62.Fi

I. INTRODUCTION

Until recently, intense narrow-linewidth radiation in the far-infrared region of the electromagnetic spectrum could only be produced with molecular gas lasers. The free-electron laser (FEL) can be a good alternative, if the effort is taken to manipulate and filter its inherently broadband spectrum. The FEL has the advantage that its wavelength is continuously tunable.

The laser process usually starts with incoherent spontaneous emission. The slippage distance $N\lambda$, where N is the number of undulator periods, determines the homogeneous bandwidth of the spontaneous emission $\Delta\nu = c/N\lambda$. The gain bandwidth is equal to $\Delta\nu = c/2N\lambda$. The spectrum of a short-pulse FEL at $\lambda = 69\mu\text{m}$ is depicted in Fig. 1(a).

The cavity length in FELs usually measures a number of meters, since the space between the two cavity mirrors should allow room for a lengthy undulator. The gain bandwidth of an FEL thus comprises a large number of cavity modes. In the case of the free-electron laser for infrared experiments (FELIX) [1], the cavity mirrors are spaced at 6 meters and the number of undulator periods is equal to 38. At an optical wavelength of 70 micrometers, this means that a total of 2300 longitudinal cavity modes are contained in the gain bandwidth. Despite these problems, narrow-line operation in several FELs has been attempted [2–4].

In the case when the FEL uses electron pulses that are substantially longer than the slippage length, gain narrowing and mode competition can lead to a narrow spectrum [2]. However, a large number of gain passes is needed to obtain a single surviving cavity mode [5]. In general, this is a problem since the electron beams are usually (except for superconducting linacs) produced during a macropulse of several microsecond that is repeated at a frequency of a few hertz.

In the case of electron pulses with lengths that are comparable to the slippage length, no gain narrowing is possible. However, by detuning the cavity length over a small amount, the length of the optical micropulses can be increased to a

coherence length of roughly 8 mm at $\lambda = 69\mu\text{m}$ in the case of FELIX. This being done, the only option that remains to reduce the number of lines in the laser spectrum is to perform phase locking [6]. To achieve this, the cavity is filled with a large number of separate optical micropulses. This is done by choosing the electron bunch repetition frequency equal to a multiple of the cavity roundtrip frequency. Phase locking is achieved by means of an intracavity interferometer that induces a strict phase relationship between the optical micropulses. The optical micropulses now act as if they were part of a much longer pulse with an effective length of many times the separation distance between the micropulses. Since the micropulses are short with respect to their separation distance, the laser spectrum still consists of a comb of frequencies that are spaced by the phase-locking frequency, see Fig. 1(b). It is the *width of these phase-locked modes* $\Delta\nu_{FS}$ that is reduced by the phase-locking process, see Fig. 1(c). The quality of the induced phase coherence determines the width $\Delta\nu_{FS}$ and hence the number of active cavity modes within this bandwidth. By phase locking, the power per mode in the FEL output spectrum is increased. The number of active cavity modes is reduced, whereas the FEL output power is, in general, unaffected.

In previous papers, the effectivity of the phase-locking method was studied for different types of intracavity interferometers. This was done both theoretically and numerically [6–8], as well as experimentally [9,4]. This paper describes an experiment in which we select a *single* line from the phase-locked spectrum of FELIX, of which the frequency can be scanned continuously.

In order to obtain a single narrow line from a FEL's phase-locked spectrum, additional filtering by means of external interferometers is required. This case is depicted in Fig. 2. The narrow lines in Fig. 2(a) correspond to the transmission function of an external Fabry-Pérot étalon that is used to filter the output signal of the laser. When we zoom in on one of these lines in Fig. 2(b), we notice that the resonant

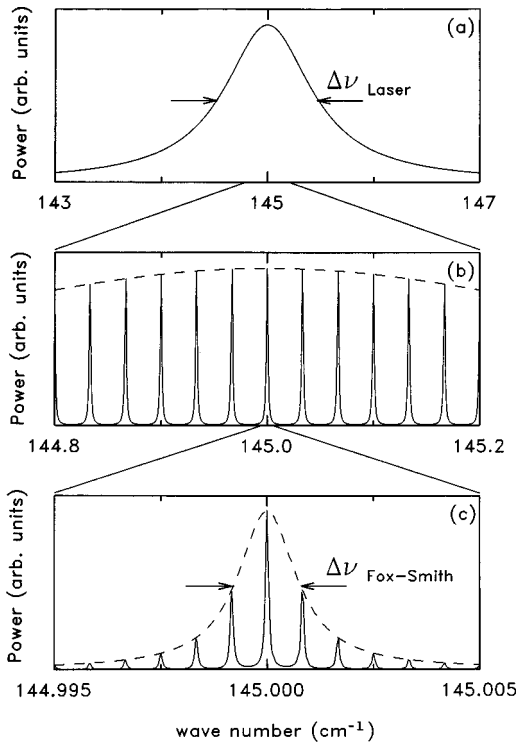


FIG. 1. The spectrum of the phase-locked short-pulse free-electron laser FELIX at three resolutions. The overall bandwidth of the laser $\Delta\nu_L$ at $\lambda = 69 \mu\text{m}$ is large, i.e., typically 1% (a). By phase locking, the spectrum is reduced to discrete lines at multiples of 1 GHz (or 0.033 cm^{-1}). Each Fox-Smith line is composed of one or more cavity modes (c). Each of the cavity modes shown in (c) belongs to a different hypermode. The quality of the interpulse phase coherence determines the width $\Delta\nu_{FS}$ of the Fox-Smith mode (c).

peak of the external étalon is narrow enough to select a *single* phase-locked mode. Again, the quality of the phase-locking process finally determines the number of cavity modes that can be consecutively or simultaneously active within the selected line, as shown in Fig. 1(c).

In a previous experiment with FELIX, the external selection was done by means of a single external interferometer [3]. The selected frequencies could not be scanned in that experiment due to the fixed distance between the plates of the external étalon.

At the Mark-III FEL Szarmes *et al.* achieved external selection of a narrow line at $\lambda = 3 \mu\text{m}$ in a similar type of experiment [4]. They gave an experimental demonstration that the resonant frequency of such a selected line could be changed. The external selection, however, was still made by means of an étalon of fixed thickness. In the experiment that is described here, we guided the phase-locked signal of FELIX through two Fabry-Perot étalons in series. The finesse of each of the étalons was equal to 23. The free-spectral ranges of the étalons were chosen in the proportion of 1:7. The effective finesse of this system was equal to 161. Thus, the suppression of undesired frequencies was improved. The étalons were designed such that the distance between the plates could be varied. Therefore, we could vary the frequencies that are resonantly transmitted by the external étalons. In order to obtain truly continuously tunable narrowband radiation, it is required to tune the resonant frequencies of the

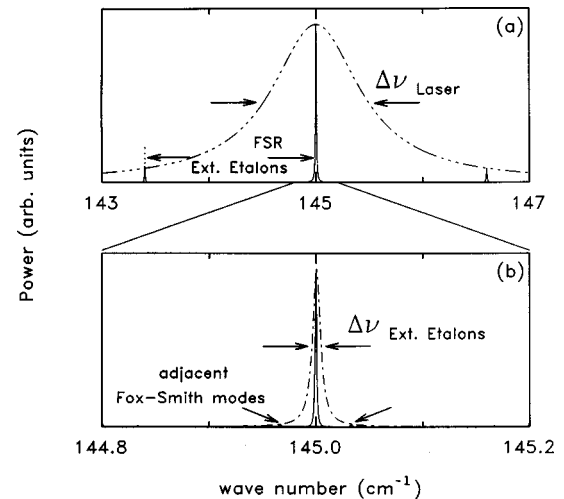


FIG. 2. The externally filtered phase-locked spectrum at two resolutions. The external étalon selectively transmits a few Fox-Smith lines from the broad laser spectrum $\Delta\nu_L$ (a). The frequency difference between the transmitted Fox-Smith lines is equal to 1.6 cm^{-1} . Due to the high resolution of the external étalon, the Fox-Smith modes adjacent to the peak in (b) [see Fig. 1(b)] at 0.033 cm^{-1} are strongly suppressed. The selected Fox-Smith line in (b) is again composed of one or more cavity modes, depending on the quality of the interpulse phase coherence, as was shown in Fig. 1(c).

FEL's intracavity étalon as well. The effects and feasibility of the latter were studied in detail in a previous article [10]. This paper gives a demonstration of high-power, continuously tunable narrow-line-width radiation that is produced with a short-pulse free-electron laser.

The outline of the remainder of this paper is as follows: In Sec. II we describe the experimental setup. Section III discusses the intra and extracavity filtering techniques that were used to produce the tunable narrow-line-width radiation. We first discuss how phase coherence is induced between the optical micropulses by means of a Fox-Smith intracavity interferometer. This is followed by a description of the properties of the external étalons. In Sec. IV the narrowband selection experiment is described. The frequency-scanning experiment is presented in Sec. V. Conclusions are given at the end of this paper.

II. SETUP

The setup of the experiment is displayed in Fig. 3. The main laser cavity consists of two gold-coated copper mirrors, M_1 and M_2 , which are separated by 6 m. The resonant frequencies of the main cavity are thus separated by 25 MHz. The upstream mirror M_1 contains a small outcoupling hole with a diameter of 3 mm. Fourty separate optical micropulses with an individual coherence length of 8 mm circulate in the main cavity of the laser. Because the amplification of the radiation occurs with a repetition rate of 1 GHz, the interpulse distance is equal to 0.3 m.

A Fox-Smith intracavity interferometer is used to induce interference between the optical fields of the subsequent optical micropulses. In the intracavity étalon the radiation bounces between the upstream mirror M_1 and the concave mirror M_3 via the partially transparent beamsplitter BS_1 . The

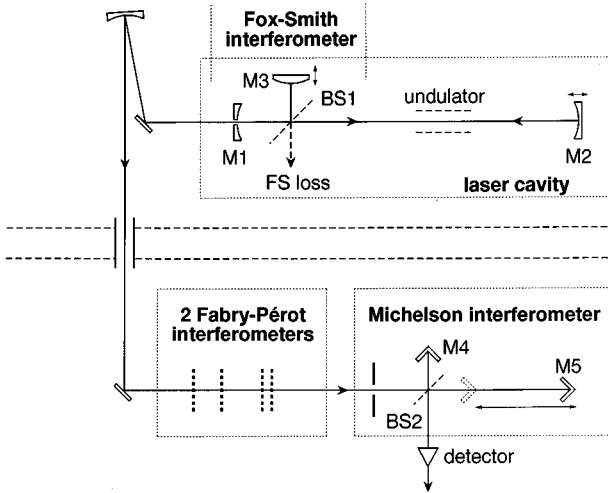


FIG. 3. A schematic of the FELIX laser cavity with the Fox-Smith intracavity étalon. The external Michelson interferometer was used for analysis.

distance L_{FS} between the Fox-Smith interferometer mirrors M_1 and M_3 is chosen approximately equal to 0.15 m. Thereby, part of the radiation of each optical micropulse temporally overlaps with that of its successors at the beamsplitter BS_1 . Due to interference, the phases of the optical micropulses become locked. The optical phase of the laser signal thereby becomes periodic over a distance of $2L_{FS} = 0.3$ m. In the frequency domain this corresponds to a spectrum with resonant frequencies that are separated by 1 GHz. This means that the majority of the cavity modes is suppressed during the gain process. Power that is contained in cavity modes that are not resonant in the Fox-Smith interferometer leaves the cavity sideways at the beamsplitter BS_1 by interference. In each set of fourty cavity modes whose resonant frequencies are found within a range of 1 GHz, only a few cavity modes can survive because their interference losses in the Fox-Smith interferometer are small enough. The selectivity of the Fox-Smith interferometer can be improved by increasing the reflectivity r^2 of the beamsplitter BS_1 . This can only be done within certain limits since the effective small-signal gain is reduced when r^2 is increased. In the case of FELIX, we cannot push this too far since the macropulse during which electron pulses are supplied to the laser has a duration of a few microseconds. We used a $12.7\text{-}\mu\text{m}$ thick polypropylene foil for the beamsplitter BS_1 , which has a power reflection coefficient of $r^2 = 0.3$ and a power transmission coefficient of $t^2 = 0.7$ at an optical wavelength of $\lambda = 70\ \mu\text{m}$. The curvature of the mirror M_3 was chosen such that the wave fronts at the beamsplitter are matched.

A small fraction of the phase-locked signal leaves the cavity by means of the outcoupling hole. It is directed through a pair of Fabry-Perot étalons, placed in series. The pair of étalons selectively transmits a single phase-locked mode from the FELIX output spectrum.

The semitransparent plates of the étalons consist of copper mesh with a grid period of $16.9\ \mu\text{m}$ and a transmitting area of 44%. The finesse of each of the étalons is equal to 23 at an optical wavelength of $70\ \mu\text{m}$. The spacings between the plates of the two étalons, d_1 and d_2 , were chosen, respectively, equal to the fractions of $1/7$ and $1/49$ of the length of

the Fox-Smith intracavity étalon L_{FS} . Thus $d_1 = 21.43\ \text{mm}$ and $d_2 = 3.06\ \text{mm}$.

The spacing of each étalon can be scanned continuously over $70\ \mu\text{m}$. This was made possible by mounting one of the étalon plates on a high-precision translation stage [11]. Deviations from the ideal parallel guidance in the form of pitch, yaw, and roll are small, the specified angular deviation being less than $10\ \mu\text{rad}$. Inside the device, the expansion of a piezoelectric crystal is used to induce the desired translation. The translation is measured by means of capacitive sensors, and controlled in a feedback loop.

The resulting narrow-line optical signal is analyzed by a Michelson interferometer and detected by a liquid-helium-cooled semiconductor germanium-gallium detector. The path difference between the branches of the Michelson interferometer can be varied between 0 and 2.1 m. Thus, the long-range coherence of the signal can be studied. The total setup operates in vacuum.

III. INTRA- AND EXTRACAVITY FILTERING

A. Phase locking

1. Theory

The theory of phase locking by means of an intracavity Fox-Smith étalon was given in a separate paper [10]. In the theory section of that paper we used the theoretical approach that Szarmes and Madey used for the case of a Michelson intracavity interferometer [7]. The most important conclusion in that work was that the system of coupled cavities (i.e., the main laser cavity with $L_c = 6.0$ m and that of the intracavity étalon with $L_{FS} = L_c/M = 0.15$ m, with $M = 40$) has M different eigenmodes, the so-called hypermodes. Each hypermode m consists of a specific comb of frequencies $f(m)$ in the spectrum of the laser:

$$f(m) = \sum_n \delta(\nu - n\Delta f_{FS} + m\Delta f_c)$$

$$\text{with } m \in \{0, 1, \dots, M-1\}, \quad (1)$$

with $\Delta f_c = 25\ \text{MHz}$, the cavity mode separation, and $\Delta f_{FS} = 1\ \text{GHz}$, the intracavity-étalon mode separation. The Fox-Smith intracavity étalon introduces losses that are different for each hypermode. The different hypermodes thus have different net gain factors, whereas the gross gain of the hypermodes is equal. The theory predicts that the hypermode with the smallest interference loss gradually becomes dominant in the laser spectrum during the macropulse. At saturation, the laser spectrum only contains the frequency comb of this hypermode. The frequency combs of the other hypermodes are suppressed. This is the principle of phase locking. By tuning the spacing of the Fox-Smith intracavity étalon L_{FS} , another resonant hypermode can be selected to become dominant at saturation.

In practice, however, the phase-locking process is influenced by the (partially) coherent spontaneous emission that is emitted by the electron bunches when they pass through the undulator [10]. The spontaneous emission, because it is partially coherent, acts as a seeding signal to the laser. The repetition frequency at which the electron bunches are in-

jected is equal to 1 GHz. Due to the specific shape of the electron bunches and due to the stability of the FELIX rf accelerator, the spontaneous emission already exhibits a considerable degree of coherence between successive pulses [12]. Therefore, the spontaneous emission signal seeds the laser at the start of the macropulse with radiation that has peaks in the frequency domain at multiples of 1 GHz [13]. Due to a small, but non-negligible noise in the optical phase of the spontaneous emission pulses, the average width of the spontaneous peaks extends over a few Δf_c , or cavity mode spacings. Moreover, due to this noise, the center and width of the spontaneous peaks in the frequency domain may vary from macropulse to macropulse, but also during a macropulse.

These variations in the seeding signal lead to the phenomenon of mode hopping, as was demonstrated in Ref. [10]: In different macropulses, different hypermodes become dominant, despite the fact that the interference losses in the Fox-Smith étalon have a minimum for one particular hypermode only. Due to the different interference losses, however, each hypermode has its own specific saturated power. For most settings in our experiment, the hopping is limited to two hypermodes. The laser then operates interleaved at two different combs of resonant frequencies, the combs being separated by the cavity mode spacing $\Delta f_c = 25$ MHz [10].

Another consequence of the partial coherence of the seeding signal is that in occasional macropulses a superposition of two (or more) hypermodes develops. In these cases, the Fox-Smith has difficulty in rejecting one of the two hypermodes. The macropulse duration of 7 microseconds is then too short to obtain a single hypermode. The resulting laser spectrum of such a macropulse contains both frequency combs.

Note that the frequency combs specified in Eq. (1) are only exact when the laser and Fox-Smith cavity lengths are equal to their synchronous lengths of 6.0 m and 0.15 m. When the lengths of these cavities are detuned by not more than a few optical wavelengths, Eq. (1) gives a reasonable approximation of the resonant frequencies of the coupled-cavity system. Strictly speaking, such a system of detuned cavities has no eigenmodes. The effect of mode pulling that occurs in this case was described in Ref. [10].

2. Simulations

A simple numerical model was used to simulate the spectrum and power of the FELIX laser during the macropulse. Details of this model are given in a separate paper [10]. The values of the input parameters that were used here are equal to those described in that paper. This simulation of the phase-locking process in a FEL takes into account the effect of partially coherent spontaneous emission. The latter was included in the model in a realistic manner: an experimental study of the characteristics of the coherent spontaneous emission in FELIX provided the necessary information to model this phenomenon [13].

In Fig. 4 we show a part of the average spectrum of a set of 48 simulated macropulses on a logarithmic scale for two different situations. Figure 4(a) gives the case of spontaneous phase locking (i.e., $r^2=0$, or without using the Fox-Smith), whereas Fig. 4(b) gives that of induced phase locking ($r^2=0.3$). Both spectra were obtained by taking the Fourier

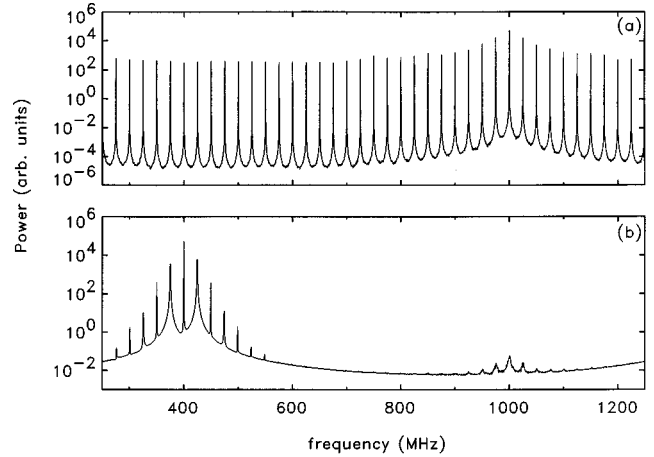


FIG. 4. The simulated average spectrum for a set of 48 macropulses. Two values for the power reflection coefficient r^2 of the Fox-Smith beamsplitter were used: $r^2=0$, or spontaneous phase-locking (a), and $r^2=0.3$, or induced phase-locking (b). The dominant resonant frequencies in (a) are found around multiples of 1 GHz, being the resonant frequencies of the spontaneously phase-locked emission. By means of induced phase locking in (b) the resonant frequencies were shifted to $n \times 1$ GHz + 400 MHz.

transform over the last 2 microseconds of the macropulses, i.e., in the saturated signal of the laser. The laser cavity was detuned by $2\delta L_c = -2.0\lambda$.

The spectrum in Fig. 4(a) is that of the laser without the intracavity étalon. It shows the cavity modes at regular intervals of 25 MHz, of which each is part of a different hypermode. On average, the cavity modes around multiples of 1 GHz are dominant in this spectrum. This is due to the fact that the spontaneous emission contains strong frequency components around multiples of 1 GHz, as was described in Sec. III A 1. Thus, without applying the intracavity interferometer to *induce* phase locking, the saturated signal of the laser is already phase locked *spontaneously*, with *fixed* dominant frequencies at multiples of 1 GHz.

By means of the Fox-Smith intracavity étalon we can select other hypermodes to become dominant. Also, the suppression of unwanted hypermodes is improved. The spectrum in Fig. 4(b) gives an example. We chose the detuning of the Fox-Smith intracavity étalon to be $2\delta L_{FS} = -0.4\lambda$, which locates the resonant frequencies of the intracavity étalon at 400 MHz + $n \times 1$ GHz. Thereby, we selected another hypermode to become dominant than the hypermodes that were preferred by the spontaneous emission in Fig. 4(a). The saturated laser spectrum in Fig. 4(b), which was averaged over 48 aselect macropulses, now has its dominant frequencies at 400 MHz + $n \times 1$ GHz. The relatively small contribution of the partially coherent spontaneous emission is still found at the frequencies of $n \times 1$ GHz. The resonant peaks that are present at regular intervals of 25 MHz from the main frequency of 400 MHz in Fig. 4(b) represent cavity modes that belong to the other, suppressed, hypermodes. The peak power in the hypermodes at 375 MHz + $n \times 1$ GHz and 425 MHz + $n \times 1$ GHz is attenuated to fractions of, respectively, 7% and 11% of the peak power in the dominant hypermode. By changing the length L_{FS} of the Fox-Smith intracavity interferometer, other hypermodes can be selected to become dominant.

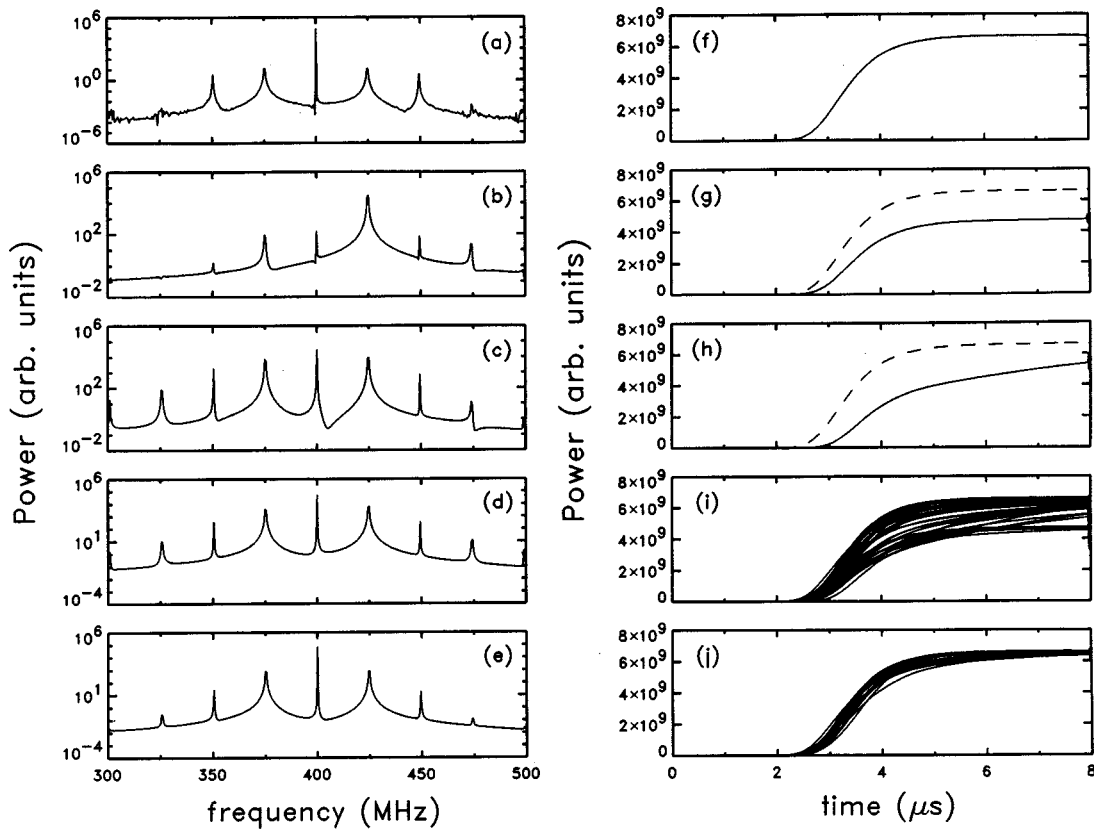


FIG. 5. (a), (b), and (c) show spectra of different individual simulated macropulses. The evolution of the laser power during these macropulses is given in (f)–(h). The signal of (f) was replotted with a dashed line in (g) and (h). (d) shows the average spectrum of 48 aselect macropulses, whereas (e) gives the improved spectrum, with respect to spectral purity, of a selection of 19 macropulses. The power signals of the 48 and 19 macropulses that were, respectively, involved in the averages are plotted in (i) and (j).

Note that the spectral lines in Fig. 4(b) corresponding to the hypermodes at $375 \text{ MHz} + n \times 1 \text{ GHz}$ and $425 \text{ MHz} + n \times 1 \text{ GHz}$ have a width that is substantially larger than that of the dominant hypermode. In general, we notice that the width of the resonant lines in Fig. 4(b) is much larger than that in Fig. 4(a). Both effects are not fully understood. Although it is to be expected that the increased interference losses that the Fox-Smith induces to certain hypermodes leads to reduced coherence lengths for these modes, it is not clear why the hypermodes at $375 \text{ MHz} + n \times 1 \text{ GHz}$ and $425 \text{ MHz} + n \times 1 \text{ GHz}$ seem to have larger widths than various other resonant lines in Fig. 4(b).

The spectrum in Fig. 4(b) was averaged over the individual spectra of 48 macropulses. The quality of this average spectrum was influenced in a negative way by two effects. These effects are caused by the influence of the partially coherent spontaneous emission, as was described in Sec. III A 1.

The first effect is mode hopping: Some macropulses operate in one hypermode, others operate in a different one. The mode hopping is, in general, limited to two to three hypermodes in the case of our experiment. The second effect is that some macropulses start to operate in a certain superposition of two (or more) hypermodes. The duration of the macropulse is in some of these cases too short to allow the Fox-Smith etalon to suppress one of these hypermodes in order to achieve single hypermode operation.

Both of the effects mentioned that deteriorate the quality of the average spectrum lead to observable differences in the

evolution of the laser output power during the macropulse. These differences can be used to make a selection of macropulses of which the average spectrum has a better quality. Single hypermode operation can be recognized by a steep increase in the output power at the start of the macropulse, while the (saturated) power has a constant level during the last microseconds of the macropulse. Macropulses that operate in different hypermodes can be distinguished mainly by the fact that their saturated output powers are different. The macropulses that operate in a superposition of hypermodes can be recognized by their impeded gain and by the fact that their power levels at the end of the macropulse still increase slowly with time. Another characteristic of these macropulses, which will not be further discussed in this text, is the fact that their power signal is modulated with a frequency of 25 MHz.

The differences are clearly observed in the simulated macropulses that are shown in Fig. 5. Figs. 5(a)–5(c) show spectra of individual macropulses from a set of 48 simulated macropulses. Figures 5(f)–5(h) show the corresponding laser powers during these macropulses. Figure 5(d) gives the average spectrum of the set of 48 macropulses (cf. a part of Fig. 4). In Fig. 5(i) the corresponding 48 macropulse signals are plotted together. Note that the sidebands in the average spectrum of Fig. 5(d) are much larger than the sidebands in the spectrum of a single macropulse like that of Fig. 5(a). In Fig. 5(a) the power contained in each of the sidebands is smaller than 0.015% of the power in the main peak, whereas in Fig. 5(d) this value is equal to 10%. Figure 5(e) gives an ‘im-

proved" average spectrum that belongs to a selection of 19 macropulses from the set of 48 macropulses. In Fig. 5(j) the corresponding 19 macropulse signals are shown. These macropulses were selected according to the criterium that their power levels at $t=8 \mu\text{s}$ should be larger than 96% of the (maximum) power level that was attained in Fig. 5(f). As is shown by Fig. 5(e), the average spectrum of the subset of selected macropulses is indeed very much improved over that in Fig. 5(d). Whereas the power contained in the sidebands at 25 MHz in Fig. 5(d) was equal to 10% of that in the main hypermode, this value is decreased to 1% in Fig. 5(e).

Such differences in the power evolution during the macropulse and in the saturation level of the laser were also observed experimentally [10]. Thus, it seems promising to select macropulses according to the described criterium for high-resolution experiments, in order to reduce the influence of the frequency and amplitude jitter that are caused by mode hopping. The macropulse output signal of the laser should then be monitored by means of a low-noise detector. The selection could be done by either a "smart-trigger" facility on the oscilloscope used in the measurement, or by suitable software after the data-acquisition. This method, however, was not used in the experiments that were described in this paper.

B. External selection

By means of filtering the phase-locked output signal of the laser, we aim to select a single frequency from the frequency comb of the induced hypermode. This can be achieved by using a Fabry-Pérot (FP) étalon as an external filter [14].

The reflective plates of a FP étalon for operation in the far-infrared region of the electromagnetic spectrum are usually made of metal mesh [15]. Commercially available electroformed mesh is suitable for wavelengths in the (sub)mm range. For far-infrared radiation around wavelengths of $70 \mu\text{m}$, this mesh is not ideally suited. However, an alternative material that can be applied for a broad range of wavelengths around $\lambda=70 \mu\text{m}$ is not available. The finesse, or resolving power, of Fabry-Pérot étalons with mesh plates is, therefore, limited at these wavelengths. We achieved a finesse of 23 at $\lambda=70 \mu\text{m}$ using copper mesh. This mesh had 1500 lines per inch, which gives a grid period of $16.9 \mu\text{m}$, while the ratio between the transmitting and the reflective area was equal to 44% [16].

Since this finesse is too small to filter a single-frequency component from the phase-locked FELIX spectrum, we used two FP étalons in series. The spacings between the plates of the two étalons, d_1 and d_2 , were chosen respectively equal to the fractions of $1/7$ and $1/49$ of the length of the Fox-Smith intracavity étalon L_{FS} , i.e., $d_1=21.43 \text{ mm}$ and $d_2=3.06 \text{ mm}$. The transmission functions of the étalons are given, respectively, in Figs. 6(a) and 6(b). Since the ratio d_1/d_2 is equal to a natural number larger than one, the transmission function of the pair of étalons approximates that of a single étalon with a larger finesse. This is depicted in Fig. 6(c). We used this configuration in our experiment. The effective finesse of the pair of étalons is equal to 161, i.e., 7 times the finesse of the individual étalons. Note that the width of the transmission peaks in Fig. 6(c) is approximately that of the

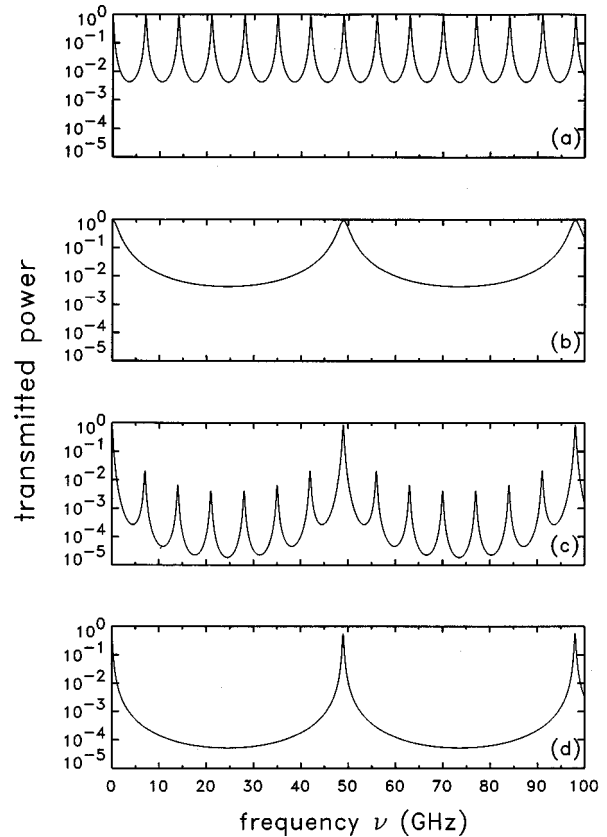


FIG. 6. The transmission spectra of several configurations of external étalons are given. (a) and (b) show spectra of the individual étalons with spacings $d_1=21.43\text{-mm}$ (a) and $d_2=3.06 \text{ mm}$ (b), where $r^2=0.87$ gives a finesse of 23. In (c) these two étalons were used in series. For comparison, (d) gives the case of a single étalon with $d=3.06 \text{ mm}$, $r^2=0.98$, and a finesse of 161.

peaks in Fig. 6(a). The latter figure represents the transmission spectrum of the external étalon with the largest plate spacing. Due to our choice of the étalon plate separations d_1 and d_2 , the effective free-spectral range of the system of the two étalons is equal to $49c/2L_{FS}$, or 49 GHz. The étalon spacings d_1 and d_2 were chosen to be rational fractions of L_{FS} because this allows a good understanding of the results when the spacings d_1 and d_2 are fine tuned in order to prepare the experiment. If we had chosen another fraction, $d_1=6.5d_2$ for example, the effective free-spectral range would have been larger.

IV. NARROW-BAND SELECTION EXPERIMENT

A. Experimental approach

At a central wavelength of $\lambda=69 \mu\text{m}$ we performed a narrow-band selection experiment. We used the Fox-Smith intracavity interferometer to obtain a phase-locked signal. The length of the Fox-Smith étalon was chosen equal to the synchronous length of $L_{FS}=150 \text{ mm}$. This was achieved by self-calibration at 1 GHz, i.e., by inducing overlap between the successive micropulses. The remaining uncertainty in $L_{FS}=150 \text{ mm}$ is discrete and equal to $\pm\lambda/2$. The cavity detuning $2\delta L_c$ was chosen equal to $-345 \mu\text{m}$. For this detuning, a relative bandwidth of 0.9% was achieved for the FELIX output spectrum.

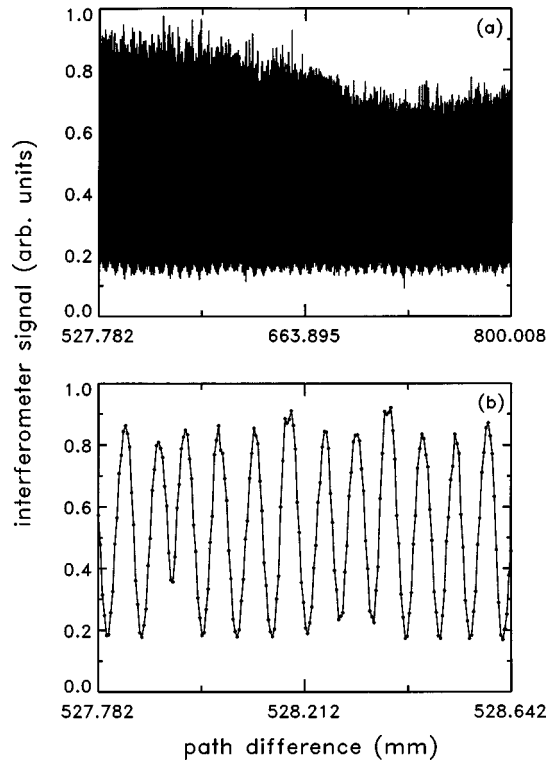


FIG. 7. The signal of the analyzing interferometer as a function of path difference. The long scan in (a) shows interference over the full length of 272 mm, which means that the external étalons selected a single phase-locked mode from the phase-locked laser spectrum. (b) shows a small piece of (a), giving the actual data points recorded for successive macropulses.

The spacings of the external étalons were chosen close to $1/7$ and $1/49$ of L_{FS} . A direct measurement of the spacings was not available. However, by optimizing the transmitted power through each of the étalons as a function of the spacings d_1 and d_2 , the specified spacings could be set to within a few wavelength's accuracy. The optimum transmission occurs only when the modes of the étalon are commensurate with as many phase-locked modes as is possible for a specific spacing. In our case, the resonant frequencies of the two étalons are commensurate with, respectively, every 7th and 49th phase-locked mode—over the full bandwidth of the laser output spectrum—since d_1 and d_2 are equal to $1/7$ and $1/49$ times L_{FS} . Since the FELIX bandwidth is finite, this method to select the spacings of the external étalons gives an uncertainty in the spacing of a few wavelengths.

We fine tuned the spacing of the étalons by means of their piezos such that a phase-locked mode in the center of the FELIX spectrum was selected. The transmitted signal of this narrow-band radiation was analyzed by means of the external Michelson interferometer.

B. Results

The result of scanning the path difference between the branches of the interferometer from 527 mm to 800 mm is displayed in Fig. 7(a). With a successful selection of a single phase-locked mode, we expect to see maximum interference over the full range of path differences in this measurement. Since the length of the long branch of the interferometer was

scanned over 272 mm, maximum interference over the full range of this interferogram would imply that the pair of external étalons succeeded in selecting a *single* phase-locked mode. Note that if more than one phase-locked mode would be transmitted by the external étalon, a decreased modulation of the interferometer signal would be observed at certain path differences along a scan of 150 mm.

However, Fig. 7(a) shows that interference occurs over the full range of the interferometer scan. Fig. 7(b) shows a small piece of this scan, indicating the period of the fringes. Each measurement point was taken in a different macropulse. Approximately 16 points were measured per path difference interval of $69 \mu\text{m}$, the length of this interval being equal to the optical wavelength. The motorized translation of the scanning mirror in the Michelson interferometer was not strictly uniform, due to irregularities in the guiding rails. Therefore, a pure sine function could not well be fitted through the data points in Fig. 7(b), and the precise wavelength of the selected narrow line could not be determined.

For a discussion of the spectrum of the selected narrow line, we will need to consider the fringe visibility at various path differences in the interferometer scan of Fig. 7(a). The fringe visibility is equal to the difference between the maximum and the minimum signal, divided by twice the average signal in the fringe. If this fringe visibility is equal to unity over a certain range of path differences ΔL_M , then the signal is 100% coherent over this range and the corresponding spectrum thus consists of a line with a full width at half maximum (FWHM) that is smaller than $1/\Delta L_M$.

There are a few complications in the interpretation of the interferogram in Fig. 7(a). First of all, we notice a decrease in the power level in the maxima for larger path differences, whereas the power level of the minima stays constant throughout the whole interferogram. This bias in the detected signal represents radiation that neither takes part in the interference, nor depends on the power of the signal that is transmitted by the étalons. The latter can be explained by the presence of straylight that bypassed the étalons in our experiment. This bias signal was stable during the full scan in Fig. 7(a) because the output power of FELIX was stable during the measurement.

Secondly, we notice a slow decrease in the signal of the maxima in Fig. 7(a). It should be noted that the measurements of Fig. 7(a) took several hours. During this time span some drifts in the lengths of the various cavities may be expected to occur. Two scenarios could explain the slow decrease in the signal of the maxima in Fig. 7(a). In the first scenario we consider a small drift in the length of the étalon with $d_1 = 21.43 \text{ mm}$. Due to such a drift, the frequency at which maximum transmission occurs in this étalon would be slightly shifted away from the (fixed) frequency of the Fox-Smith mode that is transmitted by the pair of external étalons. This shift would be smaller than 0.43 times the FWHM of the étalon peak. It would lead to a reduction in the transmitted signal of 25%, as is the case in the figure. The corresponding drift in the spacing d_1 of the étalon would be smaller than $0.7 \mu\text{m}$. Note that in this scenario the frequency of the selected narrow line would be unaffected. Only the distribution of the power over the (still small) sidebands at 0.033 cm^{-1} from this line would be slightly altered due to this drift. A drift in the length of the Fox-Smith int-

racavity étalon may also have occurred. In that case, the frequency of the narrow line would have been affected. However, we consider the latter scenario to be less likely because we did not observe such an effect in previous experiments that were performed to study the mode hopping phenomenon.

In addition to the slow decrease of the power in the maxima of the interferogram, we also notice the presence of noise in the detected maxima. Since the noise is much smaller in the minima, this is interpreted as signal noise.

There are several possible sources of signal noise in this experiment. The first is mode-hopping, see Sec. III A 2. When a new macropulse is started, the laser signal can develop in several different hypermodes. This is because the seeding signal of the partially coherent spontaneous emission that can force the laser to start up in a certain hypermode, varies from macropulse to macropulse. Since each hypermode has a different power level at which it saturates, this leads to discrete signal “noise.” Also, the combs of resonant frequencies of the different hypermodes are shifted with respect to each other by discrete steps in frequency of 25 MHz. Due to the fact that the mode hopping involves discrete hops in the frequency comb of the laser output signal, the frequency of the narrow line that is selected from this comb by means of the external étalons also hops over 25 MHz. The FWHM linewidth of the external etalon with the finest lines is equal to roughly 11 times 25 MHz. Therefore, this etalon with $d_1 = 21.43$ mm will transmit both frequencies between which the hopping occurs, but with slightly different attenuation factors. This is a second source of signal noise. Note that the frequency hopping also leads to discrete hops in the phases that are detected for different macropulses at a fixed path difference in the interferometer. At a path difference of 800 mm, a hop over 25 MHz will give rise to a phase difference of 0.13π radians. This gives rise to phase noise on the interferometer signal. However, the phase-noise affects the detected signal in the maxima and the minima equally. A third possible source of signal noise is shifts in the mean frequency of the broadband output laser signal. These shifts can be caused by jitter in the mean energy of the electrons. Since we filter a narrow line from the overall FELIX spectrum, shifts in the mean frequency of the FELIX spectrum will lead to variations in the power of the transmitted signal. The selected frequency, however, is unaffected.

If we inspect the minima in Fig. 7(a), we notice a slow modulation of the fringe depth by roughly 10% with a period of 6.05 ± 0.07 mm. This feature is ascribed to the presence of a small sideband at a frequency that is 1.65 ± 0.02 cm^{-1} smaller or larger than the dominant frequency in the obtained narrowband signal. It corresponds to a line in the tail of the FELIX spectrum, at a frequency where the external étalons are both again resonant. The free-spectral range of the pair of external étalons is equal to 49×0.033 cm^{-1} , which means that sidebands to the dominant frequency ν_c in the transmitted radiation are indeed expected at $\nu_c \pm 1.63$ cm^{-1} . Such sidebands could only be removed by using more external étalons or by reducing the width of the FELIX spectrum. The first solution will lead to a smaller power in the selected narrow-line radiation. The second is difficult to achieve with the FELIX short-pulse FEL.

To conclude, we generated a narrow-band signal by filtering the output of the phase-locked FEL. We demonstrated experimentally that the width of the selected band was smaller than 1 GHz. This means that in individual macropulses, a single cavity mode of the phase-locked laser is transmitted. Mode hopping in the phase-locked FEL determines the effective bandwidth of the signal when a series of macropulses is considered. The selected line then consists of a band of roughly 25-MHz width, in which the frequency hops between the extremes of the band.

C. Power

The average power of the phase-locked signal at $\lambda = 69$ μm , i.e., without the external Fabry-Pérot étalons, was measured in air on the optical table. It was equal to 2 mW. This power was produced by macropulses with an effective duration of 3.6 μs that were repeated at a frequency of 5 Hz. The corresponding power during the macropulse was thus equal to 111 W.

We have to take two factors into account if we want to deduce the power of the narrow linewidth radiation from this value. Firstly, we need to know the transmission factor at which each étalon passes a resonant input signal. This value was equal to 1/4 of the input power for each of the étalons. Secondly, we need to know the fraction of the input spectrum that is resonantly reflected by the pair of étalons. Since only one phase-locked mode at the center of the FELIX spectrum was selected to be transmitted, the pair of etalons reflected roughly 27/28 of the total power that was contained in the phase-locked spectrum. We thus have to multiply 111 W by 1/16 and by 1/28 to obtain 250 mW for the power that is contained in the selected narrow line during each macropulse.

This value is somewhat larger than the 100 mW that can be obtained by means of a standard far-infrared (FIR) laser. We use the FIR laser as a comparison since it is the common alternative for high-power coherent radiation in the wavelength range that is covered by the narrow-band setup at FELIX.

V. FREQUENCY-SCANNING EXPERIMENT

In an experiment by Szarmes *et al.* it was demonstrated that the output of a phase-locked FEL can be applied in high-resolution spectroscopic experiments because its resonant lines can be tuned in frequency [4]. They selected a single line from the phase-locked spectrum by means of an external grating monochromator and an external solid étalon. However, in that type of experiment the selected line can only be scanned over a limited frequency range if one requires the spectral purity of the signal to be constant during the scan.

In this section we describe the experiment in which continuously tunable, truly narrow-linewidth radiation was created with a phase-locked FEL in the far-infrared region of the electromagnetic spectrum. By means of the method that was described in Sec. IV we selected a narrow line. The frequency of this line was subsequently scanned. This was achieved by step scanning both the resonant frequencies of the Fox-Smith intracavity interferometer and the resonant frequency of the pair of external étalons.

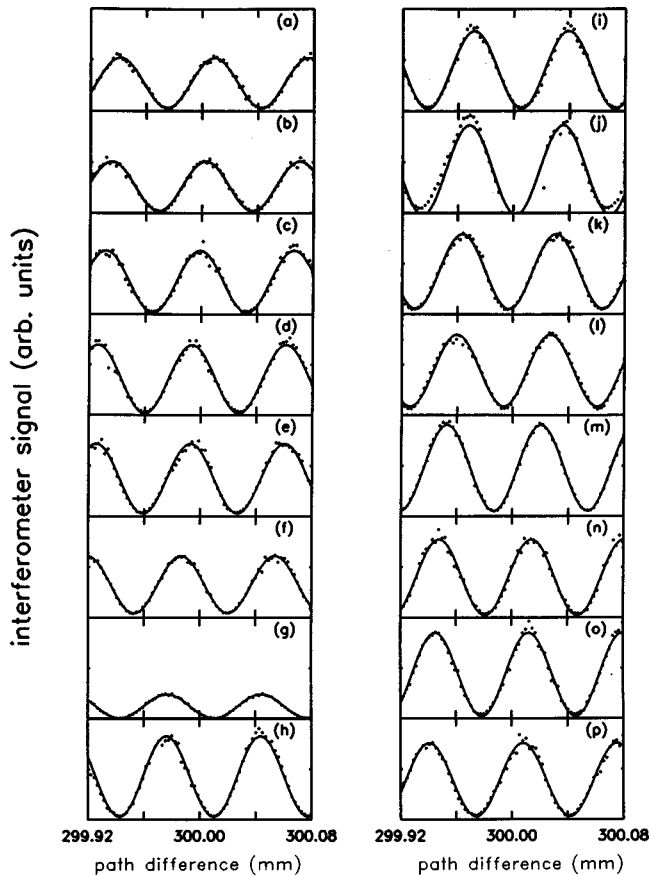


FIG. 8. Frequency scan of the narrowband radiation over 1.09 GHz in 15 steps with an average stepsize of 72 MHz. (a)–(p) show the interferograms that were measured for each step in frequency. Each data point consists of an average over the saturated signal of 20 macropulses.

A. Experimental approach

For each of 15 steps with an average stepsize of 72 MHz in the frequency of the narrow-band radiation, we measured an interferogram around a path difference of 300 mm in the analyzing interferometer. The results are shown in Fig. 8. From Figs. 8(a) to 8(p) the selected narrow-band radiation was scanned over a total range of 1.09 GHz. The interferometer signals were detected at a fixed instant during the macropulse, i.e., at saturation of the laser. Each data point in the figures consists of an average over 20 macropulses. Due to this average, the effect of mode hopping is not visible in the interferograms, although mode hopping occurred for each setting of the Fox-Smith interferometer in the experiment. Note also that the length of the laser main cavity was kept constant during the frequency-tuning experiments. Thus, the resonant frequencies of the laser cavity modes were kept fixed, being separated by discrete intervals of 25 MHz. By stepping the length of the Fox-Smith interferometer, we thus subsequently selected different cavity modes to become resonant in the laser.

The frequencies of the phase-locked modes were scanned by reducing the distance between the mirrors M_3 and M_1 . The value of L_{FS} at which the frequency scan was started was equal to 150.02 mm, modulo $\lambda/2$. The mirror M_3 was translated into the direction of the beamsplitter BS_1 in 15 steps of $2.5 \mu\text{m}$ each. Thereby, the spacing of the Fox-

Smith intracavity étalon L_{FS} was reduced by $37.5 \mu\text{m}$. At an optical wavelength of $\lambda = 69 \mu\text{m}$ the spacing was thus reduced by slightly more than $\lambda/2$. By changing L_{FS} by $-\lambda/2$ the frequencies of the phase-locked modes are scanned over a frequency range of 1 GHz, which is the free spectral range of the Fox-Smith intracavity étalon. Since we are able to scan the frequencies of the phase-locked modes over this range, we can generate any frequency—within the inherent bandwidth of the FEL—that is requested. Tuning of the frequencies of the phase-locked modes over a range larger than 1 GHz is in principle not necessary, although it is possible, according to the 1.09-GHz scan that was achieved in our experiment.

While the resonant frequencies of the laser are scanned over 1.09 GHz in steps of on average 72 MHz, the resonant frequency of the pair of external étalons should be scanned over the same frequency range with similar steps. This is achieved by scanning the spacing d_1 of the 21.43-mm étalon. Ideally, d_1 would be reduced by $5.36 \mu\text{m}$ in 15 steps of $0.357 \mu\text{m}$. For instrumental reasons, however, d_1 was scanned over $6 \mu\text{m}$ in 15 steps of $0.4 \mu\text{m}$. Thus the steps that were actually made were 13% too large. However, this did not affect the scanning of the frequency, since the exact frequency of the phase-locked mode that was transmitted by the external étalons was determined by the spacing L_{FS} of the intracavity Fox-Smith étalon. The FWHM of the finest étalon line was equal to 0.3 GHz. Therefore, despite the error of 0.13 GHz (after 15 steps) in the resonant frequency of this étalon with respect to the frequency of the transmitted phase-locked mode, the phase-locked mode is still transmitted. Only the power in the transmitted line is reduced by roughly 43%. This explains the difference between the signal levels in Figs. 8(a) and 8(o).

It was not necessary to scan the spacing d_2 of the second external étalon during the experiment. The free spectral range of this étalon was equal to 49 GHz. With a finesse of 23 this gives a FWHM of 2.13 GHz for the resonant lines of this étalon. The fine adjustment of the spacing of this étalon was chosen such that in the middle of the frequency scan, i.e., in Fig. 8(i), the frequency of the selected phase-locked mode was exactly commensurate with one of the resonant frequencies of this étalon. In Figs. 8(a) and 8(p) the frequency of the transmitted phase-locked mode was scanned by, respectively, -0.5 GHz and $+0.5 \text{ GHz}$ away from the resonant frequency of the second external étalon. These frequency differences fall well within the half width at half maximum of 1.06 GHz of the resonant lines of the second étalon. Therefore, again, the frequency scan of the narrow-band radiation itself is not affected by the choice to keep d_2 fixed during the scanning experiment. The only effect is that the selected phase-locked mode, of which the frequency is scanned, is transmitted by the second étalon with a small reduction in the power. This reduction attains a maximum of 20% in the cases of Figs. 8(a) and 8(p).

B. Results

If we compare Figs. 8(a) to 8(p), we observe that the optical phase of the detected signal—at a fixed path difference in the interferometer—shifts gradually over 1.1 times 2π , as is expected for a frequency scan of 1.1 GHz. This

means that the number of fringes that would be detected in an interferometer scan over a path difference of 300 mm, is increased by 1.1 fringe, due to the frequency scan. The latter corresponds to a relative change in the wavelength of the narrow line of $-1.1 \times 69 \mu\text{m}$ divided by 300 mm, or -0.0253% . Since $\lambda = 69 \mu\text{m}$ corresponds to a frequency of 4.35 THz, the corresponding frequency shift is equal to 1.1 GHz, as was the purpose of our experiment.

Note that the detected power in Fig. 8(g) is sharply reduced compared with the power detected in Figs. 8(f) and 8(h). For this specific spacing of the Fox-Smith intracavity étalon, the output power of the laser is sharply reduced. This effect was explained in detail in Ref. [10]. The reduced power is a consequence of the fact that the laser in this case chooses to operate in a hypermode that has larger interference losses in the Fox-Smith étalon. The reason why the laser starts to operate precisely in this hypermode, and not in the hypermode that has the smallest losses for this Fox-Smith spacing, is found in the disturbing influence of the seeding coherent spontaneous emission signal. Just in this case, the dominant frequencies of the coherent spontaneous emission are almost equal to the frequencies that are resonantly enhanced by the Fox-Smith intracavity étalon. The latter explains why the disturbing influence of the spontaneous emission signal can have such an impact for precisely this setting. If we measure the frequency with a resolution of 25 MHz, we will notice that the frequency scan is not smooth around this specific setting of the Fox-Smith spacing due to the awkward choice of the laser to operate in a hypermode with larger losses. This can be circumvented by choosing a slightly different repetition frequency of the electron bunches, by changing the frequency settings of the electron accelerator. However, the maximum amount by which the electron bunch repetition frequency can be easily adjusted is equal to 400 kHz, which might be too small for this goal. Another option is to reduce the amount of coherently enhanced spontaneous emission by manipulating the electron bunch shape [12,13]. However, this method would increase the time interval between the start of the macropulse and the instant at which saturation occurs.

C. Discussion

In the preceding text a proof-of-principle was given of the frequency scanning method. The setup is very flexible. It can also provide tunable, narrowband radiation over various other ranges of frequencies. Despite this, it cannot be prevented that the effective spectrum of the selected line will in all cases consist of two (or three) discrete lines that are separated by 25 MHz, due to mode hopping of the phase-locked FEL.

First of all, continuous scanning over a larger frequency range than 1.1 GHz is possible with the described setup. Continuous scanning over 7 GHz can be easily achieved. It involves fine scanning of the spacing d_1 of the first external étalon over $\lambda/2$, covering the full free-spectral range of 7 GHz of this étalon. Since the frequency is now scanned over a larger range, the spacing d_2 of the second étalon should now be scanned along. Considering that the free-spectral range of the second étalon is equal to 7×7 GHz, it will be clear that d_2 needs to be scanned over $1/7 \times \lambda/2$. Of course,

the frequency of the phase-locked mode that is transmitted by the external étalons also needs to be scanned. The Fox-Smith intracavity étalon has a free-spectral range of 1 GHz. This means that its comb of resonant frequencies is periodic with 1 GHz. Although a frequency scan over 7 GHz could be performed by detuning L_{FS} over 7 times $\lambda/2$, such a detuning is on the edge of what is feasible with the FELIX short-pulse free-electron laser. A better option is to detune L_{FS} of the Fox-Smith étalon from 0 to $\lambda/2$ (creating a scan of 1 GHz), and then jump back to zero detuning and start a new scan of 1 GHz by detuning over $\lambda/2$. This is to be repeated seven times. On every occasion when a new subscan of 1 GHz is started, the pair of external étalons starts to transmit a phase-locked mode that is adjacent to the phase-locked mode that was transmitted in the previous subscan. The resonant frequency of the pair of étalons then follows the frequency of this phase-locked mode during its scan over 1 GHz. The combination of the seven consecutive scans creates a frequency scan over 7 GHz.

The frequency of the narrow line can be scanned over an even wider range by fine tuning the spacing d_2 of the second étalon over $\lambda/2$. Thus, the full free-spectral range of 49 GHz of this étalon is exploited to scan the frequency. The spacing d_1 of the first external étalon should be detuned from 0 to $\lambda/2$ (covering 7 GHz), which is to be repeated 7 times. Correspondingly, the spacing L_{FS} of the Fox-Smith intracavity étalon should be detuned from 0 to $\lambda/2$ (covering 1 GHz), which is to be repeated 49 times. Since the linewidth of the FELIX output in the case of our narrowband experiments at $\lambda = 69 \mu\text{m}$ is equal to 66 GHz, it would be necessary to adjust the central frequency of the FEL a few times during the 49-GHz scan by changing the strength of the magnetic field in the undulator.

Scanning the frequency by finer steps is also an option. The smallest step that can be taken to change L_{FS} is equal to $1.25 \mu\text{m}$, which corresponds to a step in frequency of 36 MHz at $\lambda = 69 \mu\text{m}$. This stepsize is still equal to 1.5 times the cavity mode spacing of 25 MHz. Even finer tuning of L_{FS} , i.e., to achieve stepping from one cavity mode to the next, can be achieved by means of a piezoelectric crystal attached to mirror M_3 . For reliable and flexible tuning on this scale, however, the present piezo should be replaced by an expansion controlled piezo device with closed-loop control like the ones that are used in the external étalons. It is even possible to tune the frequency on a sub-25 MHz scale. This requires fine tuning of the length of the laser cavity. At this frequency scale, however, one has to realize that the effect of mode hopping causes the selected frequency to hop over discrete intervals of 25 MHz for different macropulses, see Ref. [10]. The mode-hopping phenomenon can not be prevented since it originates from the partially coherent spontaneous emission signal that is emitted by the electron bunches when they pass through the undulator. The spontaneous emission functions as a seeding signal to the laser because it is partially coherent. The mode-hopping phenomenon may limit the applicability of fine tuning on a sub-25 MHz scale in certain experiments. Nevertheless, fine tuning on this scale can be achieved. Moreover, it was shown in Sec. III A 2 that, by monitoring the power level in the output signal of the laser during the macropulse, a selection can be made of macropulses that operate in a single hypermode. By

using only the latter macropulses, the mode-hopping problem could be avoided. This would require the use of a smart trigger, which should act on the signal of the laser output power during the macropulse. The latter signal should be measured upstream of the external filtering étalons, with a low-noise detector.

VI. CONCLUSIONS

This paper described an experiment in which high-power, coherent, continuously tunable, narrowband radiation was produced in the far-infrared part of the electromagnetic spectrum. As a source we used the FELIX short-pulse free-electron laser at a wavelength of $69 \mu\text{m}$ (i.e., 145 cm^{-1}). A total of 40 micropulses were circulating in the laser cavity. Phase locking was induced between these micropulses by means of a Fox-Smith intracavity interferometer. The spectrum of the phase-locked FEL consists of discrete frequencies that are separated by 1 GHz (or 0.033 cm^{-1}), the so-called phase-locked modes. By means of a pair of external étalons, we selected a single phase-locked mode from this spectrum. This was proven by means of an interferogram in which the path difference between the branches was scanned over 272 mm. From the simulations presented, which were corroborated by previous experiments [10], it was concluded that the actual width of the selected spectral line is a fraction of the laser's cavity mode spacing of 25 MHz, or 0.00083 cm^{-1} . For individual macropulses this fraction can be very small. However, when the spectrum of the narrow line is averaged over many different macropulses, the bandwidth is much larger, due to mode hopping of the phase-

locked FEL. The effective bandwidth is then equal to 25 MHz, while the frequency of the laser hops over a discrete interval of 25 MHz between the two extrema of this band. The mode hopping originates from small changes in the properties of the partially coherent spontaneous emission, which acts as a seeding signal for each new macropulse of the laser. The average spectrum can be improved by neglecting macropulses that display a reduced saturated output power.

The frequency of the narrowband radiation was scanned over 1 GHz by scanning the spacings of the intracavity interferometer and of one of the extracavity étalons. The experimental setup also allows scanning over smaller and larger ranges. Frequency scanning over an interval of 25 MHz is feasible if the cavity length is also scanned. However, on this frequency scale one has to take the discrete jitter in the transmitted frequencies that is caused by mode hopping for granted. Despite the latter, the described experiment demonstrates that a free-electron laser can provide coherent radiation with a small spectral width and a high power in combination with an unsurpassed tunability. The power in the selected narrow line was equal to 250 mW during the macropulse of the laser.

ACKNOWLEDGMENTS

This work was supported by the Nederlandse Organisatie voor Wetenschappelijk Onderzoek (Netherlands Organization for the Advancement of Research). It is part of the research program of the Stichting voor Fundamenteel Onderzoek der Materie (Foundation for Fundamental Research on Matter).

-
- [1] D. Oepts, A. van der Meer, and P. van Amersfoort, *Infrared Phys. Technol.* **36**, 297 (1995).
 - [2] L. R. Elias, G. Ramian, J. Hu, and A. Amir, *Phys. Rev. Lett.* **57**, 424 (1986).
 - [3] D. Oepts, A. van der Meer, R. Bakker, and P. van Amersfoort, *Phys. Rev. Lett.* **70**, 3255 (1993).
 - [4] E. B. Szarmes, A. D. Madden, and J. M. Madey, *J. Opt. Soc. Am. B* **13**, 1588 (1996).
 - [5] T. M. Antonsen and B. Levush, *Phys. Rev. Lett.* **62**, 1488 (1989).
 - [6] D. Oepts and W. Colson, *IEEE J. Quantum Electron.* **26**, 723 (1990).
 - [7] E. B. Szarmes and J. M. Madey, *IEEE J. Quantum Electron.* **29**, 452 (1993).
 - [8] E. B. Szarmes and J. M. Madey, *IEEE J. Quantum Electron.* **29**, 465 (1993).
 - [9] D. Oepts *et al.*, *Nucl. Instrum. Methods Phys. Res. A* **331**, 42 (1993).
 - [10] H. Weits and D. Oepts, *IEEE J. Quantum Electron.* (to be published).
 - [11] P-750.00, Physik Instrumente GmbH, Waldbronn, Germany.
 - [12] H. Weits, C. van der Geer, D. Oepts, and A. van der Meer *Nucl. Instrum. Methods Phys. Res.* (to be published).
 - [13] H. Weits and D. Oepts, *IEEE J. Quantum Electron.* **35**, 15 (1999).
 - [14] G. Hernandez, *Fabry-Pérot Interferometers* (Cambridge University Press, Cambridge, 1986).
 - [15] K. Sakai and L. Genzel, *Int. J. Infrared Millim. Waves* **1**, 155 (1983).
 - [16] Electroformed Mesh, BMC Buckbee-Mears St. Paul, St. Paul, Minnesota.